



## NEWTONIAN FLOW MODELING THROUGH 90° PIPES BENDS

Christina G. Georgantopoulou<sup>1</sup>, Ahmed Khaled Mohamed Khan<sup>1</sup>, Nikolaos S. Vasilikos<sup>2</sup> and George A. Georgantopoulos<sup>3</sup>

<sup>1</sup>School of Engineering, Bahrain Polytechnic, Isa Town, Kingdom of Bahrain

<sup>2</sup>School of Pedagogical and Technological Education, Iraklion Attikis, Greece

<sup>3</sup>Hellenic Air Force Academy, Dekeleia Attikis, Greece

Email: [christina@polytechnic.bh](mailto:christina@polytechnic.bh)

### ABSTRACT

Flow inside pipes is extended applicable in various industrial sectors, from power plants and food industries to oil and gas companies and petrochemical procedures. In most of the cases corrosion and energy losses problems are mentioned, which are difficult to be faced due to the lack of data or information concerning the flow visualization, simulation and estimation especially at fluid flows inside sharp 90° pipes. In the present paper a flexible and accurate enough numerical approach is presented for Newtonian flows inside pipes with 90° curvature. The flow in the pipe is assumed as incompressible, laminar and viscous while the numerical results will be presented for various Reynolds numbers. Priority will be given in crude oil flows, type of Arabian light, where appropriate schemes for the prediction of the crude oil properties are developed. Existing empirical correlations as well as corresponded results by the literature are used for the needs of numerical results validation. Various results are presented concerning the flow variables, the energy losses and the stresses giving emphasis at the elbow area. It seems that near the elbow exit the stresses are increased, while maximum values are appeared on the inner radius. Additionally as the Re value is increased, more deviations occur within the stream eventually, leading to recirculation regions occurring in the pipe just downstream of the 45° section. Accurate interoperation of these deviations will show that the pressure and velocity of the fluid varies accordingly along the pipe.

**Keywords:** pipe bend flow, incompressible flow, hybrid grid, numerical modeling.

### INTRODUCTION

The numerical modelling and estimation of flows inside pipes is challenging and necessary for various industries according to the type of fluid and application. Useful results and information can be provided which can be used against pipes corrosion and erosion or for the optimization of pipes design and aspect ratio according to the type of fluid or the values of flow rates. However, the numerical model for industrial usage should not only be accurate but also simple, flexible and adjustable in order to serve the related needs. That is why we meet various computational approaches at the literature recently engaged with flows in pipes for various cases of geometry description or type of flow [1, 2]. Various types of pipes have been studied as the ones with T-junctions [3, 4] applying finite volume methodologies for single or multi flows or using the commercial software ANSYS [5]. For all the researchers and engineers is important to investigate specific regions in curved pipes or in particular non-straight pipes' parts as at Louda's [6] work for branched channels, Liu's one [7] for grooved channels, or Marn's paper [8] for the laminar flow in a 90° pipe bend. Wallini has presented an interesting numerical study for turbulent flows in compressible conditions [9]. Concerning flows inside pipes with elbows high interest presents the prediction or localization of corrosion and erosion where important numerical approaches are presented giving much information for the velocity and pressure distribution [10, 11]. Two phase flow have been also analyzed and solved (oil-water) providing very useful results especially for the oil and gas industries for the after refinery processes. [12, 13]

### Aim and objectives

Based on our previous work, concerning development of various effective numerical schemes for pipeline industrial applications [14, 15, 16], we extend our research focusing on the numerical modeling and solution of flows inside pipes with 90° elbows. This numerical investigation and estimation provide useful results for pressure drops, energy losses or separation zones inside the flow fields. In this paper an extended investigation is presented concerning flows inside sharp 90° curve pipes using uniform, un-uniform, hybrid and adaptive refined grids. We try to produce a simple and flexible scheme, easy to be applied in various industrial applications, although the mesh approach must be hybrid. The commercial software ANSYS will be used for the domain and equations discretization. Finite volume numerical schemes will be applied for the Navier-Stokes equations solution without facing in this cases any particular problem with the boundary conditions (velocity inlet and pressure outlet conditions will be applied). Energy losses, pressure coefficient estimation as well as the flow variables distribution will be specified and depicted while the differences with existing empirical correlations will be calculated and presented [8]. Additionally we will try to predict the location and the length of the separation zones, if these are developed according to the inlet velocity as well as the relationship between the inlet flow rate and the pipe diameter trying to provide the appropriate values and ratios in order to minimize the friction influence and the energy losses. Finally the pressure loss coefficient will be studied in order to investigate the relation among it and the average velocity of the pipe.



## THEORETICAL ANALYSIS AND NUMERICAL METHODOLOGY

The energy losses and the friction influence in a pipe bend have been extended studied experientially and various empirical formulas have been extracted. In order to study the flows in curve pipes the Dean number is defined as follows:

$$De = \frac{\rho V d}{\mu} \sqrt{\frac{d}{2R_c}} \quad (1)$$

where  $De$  is the Dean number,  $\rho$  and  $\mu$  the density and the dynamic viscosity of the fluid respectively,  $V$  the velocity of the fluid,  $d$  the diameter of the pipe and  $R_c$  the curvature radius. The Dean number is in fact a connection between the radius of the pipe and the curvature radius. Using this dimensionless number the following formula can be used in order to calculate the friction coefficient in curvature [8]:

$$\frac{f_c}{f_p} = 1 + 0.033(\log De)^4 \quad (2)$$

where  $f_c$  the friction coefficient in curvature,  $f_p$  the Fanning friction coefficient and  $De$  the Dean number as stated above. The Fanning friction coefficient is calculated as follows:

$$f_p = \frac{16}{Re} \quad (3)$$

where  $Re$  is the Reynolds number.

By this way, or using other similar correlations, empirical calculations can be achieved providing an approach concerning the related energy losses.

### Crude oil properties

The computational approach which follows is applied but not limited to crude oil flows. Crude oil is complex composite that contains several components presenting high chemical reactions and thermal variations in many specific conditions. The crude oil depends on the geographical source, the chemical consistency and its composition is not stable. Many research works have been developed trying to calculate by various ways the flow properties of the crude oil according to the mixture, the temperature and various other conditions [17, 18, and 19]. As a result for this issue the American Petroleum Institute "API" has classified the different types of crude oil, the degree for measuring and classifying the crude oil is "API" which has its own formula. In order to classify the type of crude oil, the viscosity and "API" degree are important parameters although their specific calculation varies according to the methodology. However, we are interested in the crude oil that is coming from Saudi Arabia to the main line of Bahrain so the crude oil type is light and the API value of the Saudi Arabia - Arabian light according to the Energy Information Administration is 34.2 while according to [19] the API value must be between 20 to 48 for Middle east crude oil. Choosing the

Elsharkawy-Alikhan [17] methodology in order to calculate the viscosity, we apply the following formulas:

$$\mu = \text{antilog}_{10}(x) - 1 \quad (4)$$

$$x = \text{antilog}_{10}(y) \quad (5)$$

$$y = 2.1694 - 0.02525API - 0.68875 \log_{10}(T) \quad (6)$$

where the dynamic viscosity can be predicted according to the operating constant temperature  $T$ . Following the above procedure we choose to use as properties values as these are presented below:

Dynamic viscosity,  $\mu = 0.009137296 \text{ kg/(m.s)}$

Kinematic viscosity,  $\nu = 0.0000107 \text{ m}^2/\text{s}$

Density,  $\rho = 853.9529 \text{ kg/m}^3$  [20].

### Assumptions

In order to study the crude oil behavior using the above (4-6) equations, we apply the following assumptions:

- The fluid is Newtonian and incompressible
- The fluid presents constant chemical properties
- There is no temperature variation during the flow.
- There are no chemical reactions during the flow.

### Numerical methodology

In order to produce the computational modeling for the aforementioned flow, FLUENT is used for all the steps of CFD procedure. Uniform and un-uniform hybrid grids have been applied in combination with control volume methods and implicit schemes.

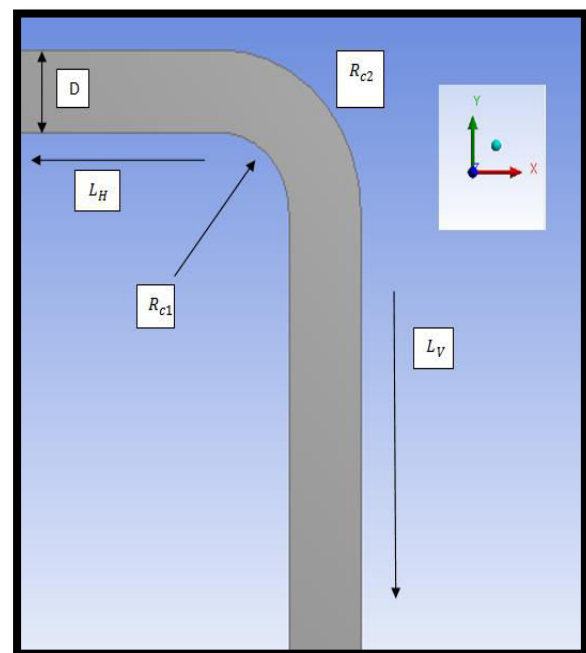


Figure-1. Pipe with elbow: geometry description.



We have calculated the above geometry when the diameter of the pipe is equal to the radius of the inner curvature.

**Mesh generation and geometry description**

The geometry of the pipe with certain characteristics is depicted at Figure-1. As it is stated at the Figure below two types of lengths have been defined  $L_H$  before the elbow and  $L_V$  after it. By the other hand,  $R_{C1}$  and  $R_{C2}$  are the internal and external radius of the elbow respectively. We have calculated the above geometry when the diameter of the pipe is equal to the radius of the inner curvature. The specific dimensions are presented at table 1 as it can be seen below:

**Table-1.** Dimensions of the physical geometry.

Symbol	(m)
Diameter	0.7620
$L_H$ (x channel, before elbow)	4.0000
$R_{C1}$ Internal radius of curvature	0.7620
$R_{C2}$ External radius of curvature	1.4960
$L_V$ (y channel, after elbow)	5.0000

The type of mesh is used for this design, it is a hybrid mesh. Although according to our previous research [21, 22], the Cartesian grid generation approach is more simple and flexible, in this work we prefer the hybrid grid application as a first approach, paying more attention to the maximum shear stresses localization. In our near future research the Cartesian grids methodology will be developed for the specific flow.

Since this is a 90° pipe bend design, there will be a x-channel followed by a bend and finally leading into a straight pipe (y-channel). For the x and y-channels a Cartesian mesh, which is easily developed for linear components, has been generated, while the bend will be covered by a body fitted mesh which has been set as an adaptive type regarding the curvature (Figures 2 and 3). Moreover, whenever the geometry of the bend is updated, the mesh will also be updated and optimized by the software.

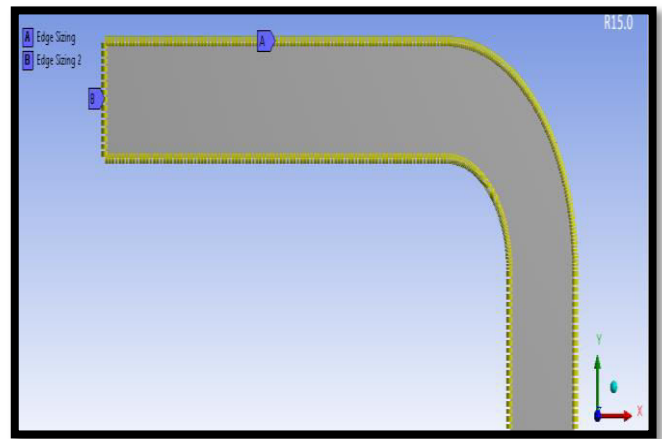


**Figure-2.** Edge sizing of the two groups; group (A) is of the pipe's linear components and the bend, while group (B) is the inlet and the outlet. The divisions have been clustered at the bend to insure accurate results.

The elements of the mesh have been scaled using the edge sizing option in the software. Using this feature the components have been split into the linear components (x and y-channels) and the pipe bend into one group, while the inlet and outlet in a separate group.

**Table-2.** Mesh data.

Mesh specifications	
Group (A): the x and y-channels and the pipe bend	350 divisions
Group (B): the inlet and the outlet	30 divisions
Number of elements or cells	31500 cells
Number of nodes	65162

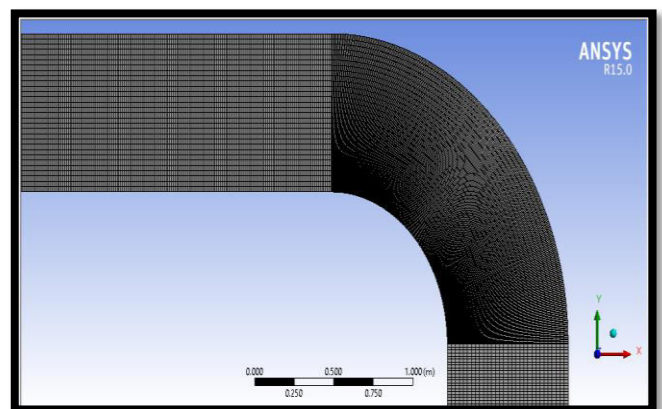


**Figure-3.** The used Hybrid grid. The vertical and horizontal pipe section contains a Cartesian mesh while the pipe bend contains a body-fitted mesh.

**Governing equations**

The governing equations are the Navier – Stokes, as you can see below, which in combination with the mass



conservation equation (continuity) provide the desired flow domain solution:

$$\frac{\partial \rho}{\partial t} + \frac{\partial(\rho u)}{\partial x} + \frac{\partial(\rho w)}{\partial y} + \frac{\partial(\rho v)}{\partial z} = 0 \tag{7}$$

Mass conservation:

Momentum equations:

$$\frac{\partial(\rho u)}{\partial t} + \frac{\partial(\rho u^2)}{\partial x} + \frac{\partial(\rho uv)}{\partial y} + \frac{\partial(\rho uw)}{\partial z} = -\frac{\partial p}{\partial x} + \frac{1}{Re} \left( \frac{\partial \tau_{xx}}{\partial x} + \frac{\partial \tau_{xy}}{\partial y} + \frac{\partial \tau_{xz}}{\partial z} \right) \tag{8}$$

$$\frac{\partial(\rho v)}{\partial t} + \frac{\partial(\rho uv)}{\partial x} + \frac{\partial(\rho v^2)}{\partial y} + \frac{\partial(\rho vw)}{\partial z} = -\frac{\partial p}{\partial y} + \frac{1}{Re} \left( \frac{\partial \tau_{xy}}{\partial x} + \frac{\partial \tau_{yy}}{\partial y} + \frac{\partial \tau_{yz}}{\partial z} \right) \tag{9}$$

$$\frac{\partial(\rho w)}{\partial t} + \frac{\partial(\rho uw)}{\partial x} + \frac{\partial(\rho vw)}{\partial y} + \frac{\partial(\rho w^2)}{\partial z} = -\frac{\partial p}{\partial z} + \frac{1}{Re} \left( \frac{\partial \tau_{xz}}{\partial x} + \frac{\partial \tau_{yz}}{\partial y} + \frac{\partial \tau_{zz}}{\partial z} \right) \tag{10}$$

Where  $\rho$  is the density,  $t$  the time,  $u$ ,  $w$  and  $v$  the velocity components,  $x, y, z$  the Cartesian coordinates,  $Re$  the Reynolds number,  $p$  the pressure and  $\tau$  the shear stresses. Our modeling is 2D, for laminar, incompressible, viscous and steady flows. Consequently the above equations are transformed accordingly to the flow conditions as well as the initial conditions provide the desired flow characteristics. The flow solver is the SIMPLE applying a second order upwind scheme for the spatial discretization. The under relaxation factors are chosen between 0.3 to 0.7 in order to provide better stability to our final numerical solution [5, 20].

**Boundary conditions**

The appropriate choice of the boundary conditions in every numerical approach is fundamental and determinative for the accuracy precedence of the results [23, 24].

In order to develop the computational calculation of the flow fields the appropriate boundary conditions have been set according to the geometry of the physical bound (Figure-1). At the inlet conditions, the velocity profile is given while at the outlet of the pipe Neumann conditions have been applied for the velocity and Dirichlet for the pressure. Along the wall of the pipe, no-slip conditions have been set in order to provide the zero value for the velocity. The boundary conditions can be seen at the table. The appropriate lengths ( $L_H$  and  $L_V$ ) have been set to the appropriate values in order the fully developed flow to be created before and after the bend. Its worth to be mentioned that these lengths are depended on the Reynolds number values.

**Table-3.** Boundary conditions.

Inlet	<b>Inlet conditions giving the value of the velocity:</b> $u = u_{ref}, w = 0, \frac{\partial p}{\partial x} = 0$
Outlet	<b>Outlet conditions where pressure is given:</b> $u = 0, \frac{\partial w}{\partial y} = 0, p = 0$
Upper bound	Wall conditions: $u = w = 0, \frac{\partial p}{\partial y} = 0$
Lower bound	Wall conditions: $u = w = 0, \frac{\partial p}{\partial y} = 0$

**RESULTS**

As we have already mentioned the incompressible flow inside the 90° bend pipe will be presented. The calculations have been achieved for three different values of Reynolds number, 100, 750 and 1500 where the related inlet velocities as well as some more computational data concerning the flow characteristics are presented at Table-4.

The properties of the fluid have been already been described above; while the mesh which has been applied is hybrid according to the physical domain demands (Figure-3). For all the various test cases that we have performed, the mass flow rate is concerned as the difference inlet and outlet of the pipe is always less than  $5 \times 10^{-6}$ .

**Table-4.** Inlet velocity values.

Re number	Velocity (m/s)	De	Velocity max (m/s)	Mass flow rate (kg/s)
100	0.003045	70.7100	0.00455	2.0000
750	0.022800	530.330	0.03100	14.976
1500	0.045670	1060.66	0.05800	29.998

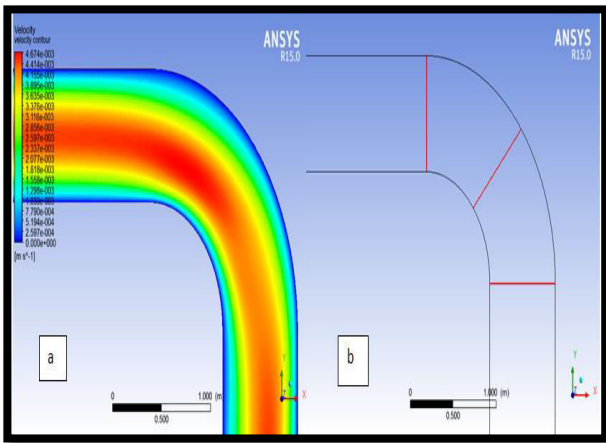


**Figure-4.** (a) Velocity contour where it has been focused on the bend. (b) The three different locations were lines have been set for to generate velocity profiles; the lines are set before, along and after the bend.

We present the velocity contours close to the bend for the three different cases of Reynolds number trying to depict the flow distribution variations. At Figure-4 the velocity distribution along the bend is presented when the Reynolds number has been set equal to 100 while at Figure-5 the pressure distribution along the pipe.

The fluid enters with a maximum velocity of 0.003045 m/s. The velocity contour shows a color scheme ranging from 0.0028-0.0031 m/s, in accordance to the inlet velocity. Some interesting results are presented through the pressure distribution along the bend. The outer curvature of the bend shows a high concentration of pressure reaching 0.011 Pa, while the inner curvature has a low pressure of 0.0042 Pa. According to the relationship pressure - velocity the distribution of the results seems reasonable and acceptable.

At Figure-6 comparisons between the velocities distribution along the pipe is presented for two different Reynolds numbers, 750 and 1500. The contours show that with the increase of the Re value and in turn the velocity, the fluid flows with a higher fluid inside the pipes causing it to deviate after the bend. This is present in the contour showing the results for Re 750. At Re 1500 the stream develops a region at which recirculation occurs. These are the point where the flow is separated by the wall and maximum shear stress is expected. It cannot be said precisely, but we believe that in such locations, corrosion is more possible to happen.

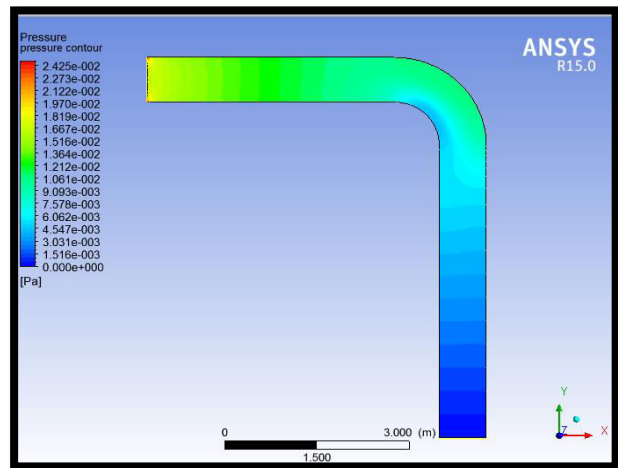
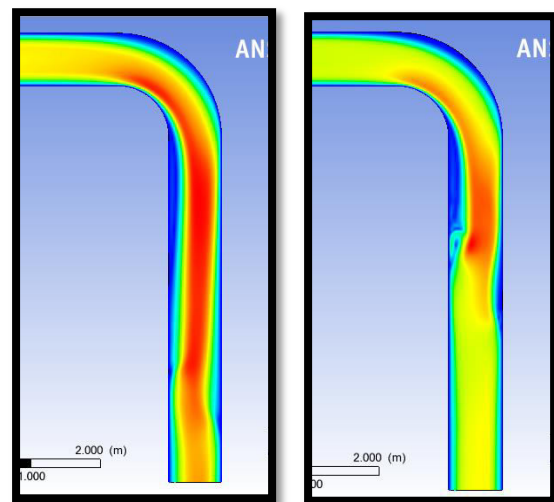


**Figure-5.** Pressure distribution along the pipe. Re=100.



(a) (b)

**Figure-6.** Velocity contours for (a) Re=750 and (b) Re=1500.

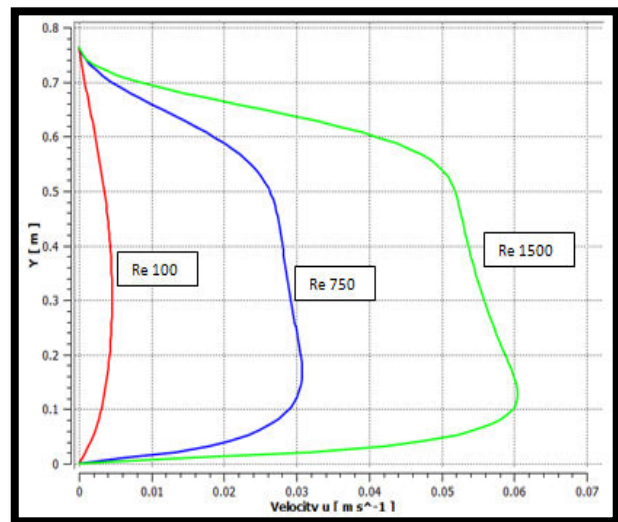


**Figure-7.** Velocity profiles before the fluid enters the bend. Re=100, 750, 1500.

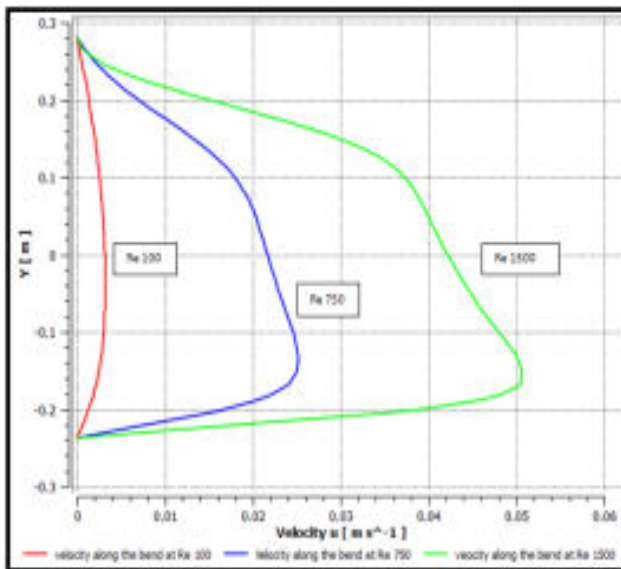


**Figure-8.** Velocity profiles along the bend.  $Re=100, 750, 1500.$

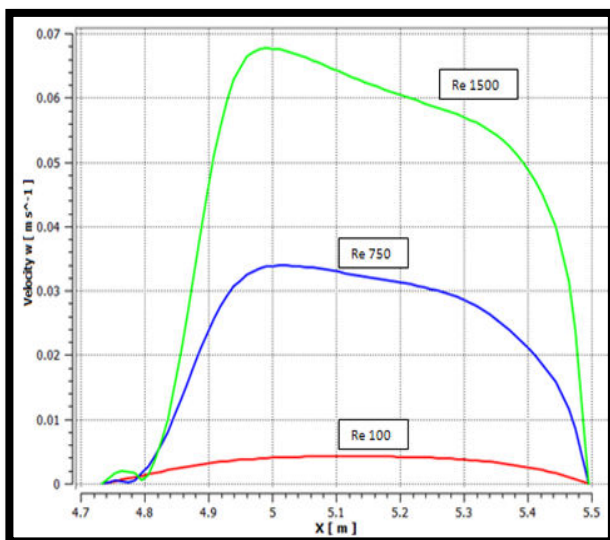


**Figure-9.** Velocity profiles while the fluid exits the bend.  $Re=100, 750, 1500.$

Interesting distribution is appeared at the Figures 7, 8 and 9 where the velocity profiles before, along and after the bend is presented for three different values of Reynolds numbers. The influence of the Reynolds number is significant, not only to the velocity maximum values, which is reasonable, but also at the variation of the flow along the pipe close to the bend section. That is why, as we can see at Figure-6, a brief separation zone is appear close to the inner wall of the pipe when the Reynolds number is equal to 1500. Through the various test cases that we have developed, we have found that the separation zone starts clearly to be developed after Reynolds number equal to 1000, while even a little bit earlier ( $800 < Re < 1000$ ) a disorder to flow is visible. Through these results the exact location and the expanse of the

separation zones can be predicted as well as useful results for the pipe flow control and maintenance systems.

## CONCLUSIONS

The numerical analysis and estimation was conducted for a crude oil flow through a  $90^\circ$  pipe bend. The analysis has been conducted on three different  $Re$  values (100, 750 and 1500) which in turn impacted the inlet velocity of the fluid (0.003045, 0.0228 and 0.4567 m/s). The properties of crude oil that went into the simulation were determined using a correlation linking the density, dynamic and kinematic viscosity of different grades of crude oil, while the Arabian light one has been chosen with API equal to 32.8 native to the Middle East oil product. A hybrid mesh was generated for the physical domain discretization due to the nature of the bounds. The final results collected from the numerical analysis showed that irregularities arise in the stream as the  $Re$  value is increased. With  $Re$  750 a deviation in the stream occurs after the bend, while at  $Re$  1500 recirculation regions occur after the bend. The certain location of the separation flow points has been depicted and it seems that in this region, maximum shear stresses are expected. It cannot be said precisely, but we believe that in such locations, corrosion is more possible to happen. However through the results it seems that corrosion cannot normally be expected at the outer radius of the pipe as the maximum stresses seem to be developed only close to the inner pipe bound after the bend. The data can also be used to conform between pumping stations and oil refineries to detect any changes in the flow of crude oil inside of bend in pipes. Future research will be done considering higher Reynolds numbers with parallel introduction of a turbulent model.

## REFERENCES

- [1] Kaiktsis L., Karniadakis G.E., and Orszag S.A. Onset of three-dimensionality, equilibrium, early transition in flow over a backward-facing step. *Journal of Fluid Mechanics*, 501–528, 1991.
- [2] Razavi S., Hosseinali M., A review of pressure behavior after a backward – facing step, *Recent advances in Fluid Mechanics*, pp. 52-58, 2009
- [3] Louda P., Kozel K., Prihoda J., Benes J., Kopacek T., Numerical solution of incompressible flow through branched channels, 46 (2011) 318-326.
- [4] Phan H., Wen L., Zhang H., Numerical simulation and analysis of gas liquid flow in a T-junction micro channel, *Advances in Mechanical Engineering*, (2012), ID 231675.
- [5] Shamloo H., Pirzadeh B., Investigation of characteristics of separation zones in T-junction



- channels, WSEAS transactions on Mathematics, 7 (2008) 303-312.
- [6] Louda P., Kozel K., Prijoda J., Benes L., Kopacek T., Numerical solution for incompressible flow through branched channel”, *Comput. Fluids*, vol. 43, pp. 268-276, 2013.
- [7] Liu C., Liu Z., McCormic S., “Multilevel adaptive methods for incompressible flow in grooved channels”, *J. of Computational and Applied Mathematics*, vol. 38, pp. 283-295, 1991.
- [8] Marn J., Ternik P., “Laminar flow of a shear thickening fluid in a 90o pipe bend”, *Fluid Dynamics Research*, vol. 38, pp. 295-312, 2006.
- [9] Wallin S., Johansson A.V., “A complete explicit algebraic Reynolds stress model for incompressible and compressible turbulent flows”, *Journal Fluid Mechanics*, vol. 403, pp. 89-132
- [10] Christofer B.S., Wong C.Y., Boulanger J., “An experimental and numerical analysis of erosion caused by sand pneumatically conveyed through a standard pipe elbow”, *Wear*, vol. 336-337, pp. 43-57
- [11] Tijsseling A., Vardy A., Fan D., “Fluid structure interaction and cavitation in a single-elbow pipe system”, *Journal of Fluids and Structure*, vol. 10, pp. 395-420.
- [12] Pouraria H., Paik K., Seo K., “Modeling of two - phase oil/water flow in horizontal pipeline using CFD technique, Proc. Of the Int. Conference on Offshore mechanics and Arctic Engineering - OMAE, France, 2013.
- [13] Yang D., Wang X., Xiao S., Zhang D., Chen X., “Analysis of stream injection profile in horizontal well for heavy oil recovery”, *Journal of China University of Petroleum*, vol. 38, pp.155-159, 2014
- [14] Georgantopoulou C., Georgantopoulos G., Vasilikos N., Saw tooth approximation and numerical solution for flow in inclined channels, *WSEAS Transactions on Fluid mechanics*, 10(2015) 69-79.
- [15] Georgantopoulou C., Georgantopoulos G., Vasilikos N., Numerical analysis and modeling of recirculating flows, *Int. Journal of mathematical Models and Method in Applied Sciences*, 9(2015) 248-260.
- [16] Georgantopoulou C., Georgantopoulos G., Vasilikos N., Local Refinement approach for incompressible developing flows inside pipes”, *Int. Conference on Applied Physics and Mathematics, ICAPM16, Athens, Greece.*
- [17] Elsharkawy AM., Alikhan A., Models for predicting the viscosity of Middle east crude oils, *Fuel*, 78 (1999) 891-903.
- [18] Minero F., Sanchez-Reyna G., Ancheyta J., Marroquin G., Comparison of correlations based on API gravity for predicting viscosity of crude oils, *Fuel*, 138 (2014) 193-199.
- [19] Alomair O., Esharkawy A., Alkandari H., A viscosity prediction model for Kuwaiti heavy crude oils elevated temperatures, *J. of Petroleum Science and Eng.*, 120 (2014), 102-110.
- [20] C. Georgantopoulou, Feras Ali, N. Vasilikos, G. Georgantopoulos, “Numerical modelling and investigation of crude oil flow in T-junction channels”, *Applied Mechanics and Materials*, vol. 829, pp. 15-21, (2016).
- [21] Georgantopoulou C., Vasilikos N., Georgantopoulos G., “Mathematical modelling for the solution of incompressible flow through channels using block structured grids”, *WSEAS MAMECTIS14, Lisbon, Portugal.*
- [22] Georgantopoulou Chr., Georgantopoulos G., Vasilikos N. and Tsangaris S., “Cartesian refinement grid generation and numerical calculation of flows around Naca0012 airfoil” *Proceedings of Int. Conference on Applied mathematics, simulation, modelling.* pp. 256-263.
- [23] Chr.G. Georgantopoulou and S. Tsangaris, “Block mesh refinement for incompressible flows in curvilinear domains”, *Applied Mathematical Modeling.* Vol. 31, pp. 2136-2148.
- [24] Mavromatidis L., El Mankibi M., Michel P., Santamouris M., Numerical estimation of time lags and decrement factors for wall complexes including multilayer thermal insulation in two different climate zones, *Applied Energy.* vol. 92, pp. 480-491, 2012.